A Numerical Analysis of Internal Radial Clearances on Affecting Vibration of Rolling Element Bearings with Local Defects

Minmin Xu[1,2], Yimin Shao[1(✉)], Yaoyao Han[1,2], Fengshou Gu[2], and Andrew Ball[2]

[1] State Key Laboratory of Mechanical Transmission, Chongqing University, Chongqing 400044, People's Republic of China
ymshao@cqu.edu.cn
[2] Centre for Efficiency and Performance Engineering, University of Huddersfield, Huddersfield H1 3DH, UK

Abstract. Rolling element bearing is an essential component in rotating machines and its condition monitoring has attracted much concern in past decades. Bearing vibration response analysis will provide theoretical basis for fault diagnosis and maintenance of the machinery. In view of bearing usually go through various wear during operating process, resulting in increase of clearance, this paper presents a nonlinear bearing vibration model of deep groove ball bearings to explore the vibration responses affected by bearing internal radial clearance, rotational speed and external load, as well as the diagnosis features for condition monitoring. A nonlinear dynamic model with six degrees of freedom was established at first. Then, numerical simulation was implemented. Lastly, a comprehensive analysis from time domain and frequency domain were carried out based on statistical indicators and spectra. Numerical results show that information from frequency domain outperforms statistical indicators from time domain for bearing clearance monitoring. To bearings with local defects on outer and inner races, the ball pass frequency of outer race (BPFO) and ball pass frequency of inner race (BPFI) shows uptrends with the increase of bearing clearances in general, respectively. However, there are fluctuates in BPFI for inner race fault, which needs special care in fault detection. Besides, spectral centroid has better performance on monitoring clearances of bearing with local defects. All these findings provide theory and data support for bearing fault diagnosis at an early stage.

Keywords: Rolling element bearing · Radial clearance · Nonlinear dynamic model · Hertzian contact deformation · Condition monitoring

1 Introduction

Rolling element bearings are vital parts in rotating machines, such as wind turbine, train and heavy equipment. Complex working conditions and harsh environment may cause faults on bearings, leading to fatal breakdowns, catastrophic accident and economic losses. Hence, for the reduction of faults and losses, many engineers and scholars

D. Zhen et al. (Eds.): IncoME-V 2020, MMS 105, pp. 1–13, 2021.
https://doi.org/10.1007/978-3-030-75793-9_1

have paid considerable attention on the health condition monitoring of rolling element bearings in nowadays [1].

Once a local defect, such as spall on raceways, appears on bearing, it will tempt an impact to the whole bearing vibration system. And then, resonant frequencies of the bearing parts and neighbouring components could be excited by the impulse [2]. Based on this, a large volume of research works have focused on fault detection through vibrational signal analysis with the acquired vibration data [3–5]. It has been proved to be a valid approach to realize fault diagnosis for bearings and most rotating machines. However, these signal processing methods are based on some foundational knowledge of mechanical structure and vibration mechanism, such as fault characteristic frequencies. On the other hand, mechanism analysis is an effective tool to reveal the mechanism behind the mechanical structure and obtain the representation form of fault. Usually, through establishing a dynamic model, characteristics of the system could be obtained [6, 7]. It is the basis of mechanical fault diagnosis, which provides foundation for data-driven methods. In this study, model-based method is utilized to explore the vibration characteristics of bearings influenced by bearing internal radial clearances.

Internal radial clearance means the clearance between the raceways and ball in a ball bearing. The bearing clearances have a critical impact on bearing operating temperature, system vibration and rotating life. Thus, it is a key factor for bearing selection. Investigations show that bearing usually go through various wear and tear during operating process, which results in the increase of clearance [8]. Besides, bearing clearance is an vital factor on bearing load distribution, which has a significant influence on the fatigue life of rolling bearings [9, 10]. Especially, investigation shows that wear and tear in the operating process shorten bearing rotating life by about 30% [11]. Consequently, it is urgent to study the mechanism of bearing internal clearances.

Bai et al. [12] presented a general rotor dynamic model for studying the dynamic properties considering the impact of bearing clearance and raceway waviness. Harsha [13] investigated the nonlinear characteristics of a balanced rotor with bearing internal radial clearance and detected the chaotic responses. Upadhyay et al. [14] studied the behavior of an unbalanced rotor affected by radial internal clearance of the supported bearings and high rotating speed. Zhuo et al. [15] utilized a vibration model to analyse the dynamic properties of the ball bearing as a result of applied load, waviness and internal clearances during the process of start and constant speed operation. Even a large number of literatures could be found focusing on bearing clearance through model-based methods, comparatively little scholars studied on different bearing clearances on vibrational responses. Nevertheless, sufficient acknowledge on vibration characteristics under different clearances will be benefit to account for various vibration phenomena and bearing clearances monitoring.

On mechanism of bearing clearance, Oswald [11] investigated the bearing load distribution and fatigue life under the effect of four different level of internal radial clearances on ball and roller bearings with radical load. Recently, Rehab et al. [16] presented a nonlinear dynamic model to investigate the diagnostic features under two group bearing clearances and point out that inconsistency on bearings with inner race defect according to characteristic frequency amplitude. More recently, the author Xu et al. [17] proposed a six degrees of freedom (DOF) dynamic model to study the vibration behavior influenced

by continuously changing bearing clearances and working conditions, including external load and rotating speed. It is pointed out that ball pass frequency of outer race (BPFO) dominates the envelope spectrum for bearing before obvious local defect on raceways. On the other hand, to monitor the bearing clearances, Zmarzły [18] pointed out that medium frequency band, from 300 Hz to1800 Hz, has the biggest effect on bearing vibration level under different radial clearances through experiment study. Georgiadis et al. [19] predicted bearing clearance variations with spectrum kurtosis by test vibration data. Yakout et al. [10] investigated the relationship between the clearance and bearing system damping characteristics. Meier et al. [20] utilized kurtosis, recurrences and neural networks three methods to measure the clearances through experiment test and obtained a correlation between bearing clearance and vibration level. Recently, Wang et al. [21] utilized modulation signal bispectrum (MSB) to extract features and combined with Gini-index to monitor the variation of bearing clearances online, which show that useful information extracted from frequency domain is effective on detecting bearing clearances. Besides, in previous work (Ref. [17]), we have proposed a bearing vibration model to study the bearing vibration responses with different clearances and working conditions. Both RMS and spectral centroid increase with the radial clearance in general but some local fluctuations [17]. However, in some cases, there are local defects on bearings, such as outer race and inner race fault. When local defect appears, bearing will enter the period of failure rapidly and the vibration responses are different from bearing without faults, which brings much difficulty for online monitoring of bearing clearances.

In this study, a nonlinear bearing vibration model is utilized to explore the vibration responses under various clearances with and without local defects on bearing raceways. Firstly, bearing dynamic equations are derived through is established. Then, simulation results are provided. Last, comprehensive analyses are carried out to display the difference between fault-free bearings and faulty bearings for bearing clearance monitoring.

2 Bearing Vibration Numerical Model

2.1 Bearing Clearances

Internal clearance is the geometrical clearance between the races and ball in a ball bearing. The diagram of bearing radial clearance is presented in Fig. 1.

According to the ISO standards and bearing manufacturer, the internal radial could be classified into five classes for deep groove ball bearing [9]. Table 1 represents the minimum and maximum of different level of clearance. It should be noted that the clearances shown in the table are the original values after manufacturing.

2.2 Bearing Vibration Model

To monitor clearance, a vibration model is developed with six DOF, as shown in Fig. 2. In this shaft-house system, X, $\dot{X}$ and $\ddot{X}$ represents the displacement, velocity and acceleration in X direction, respectively. s, h and r denote shaft, housing and sensor in the bearing system.

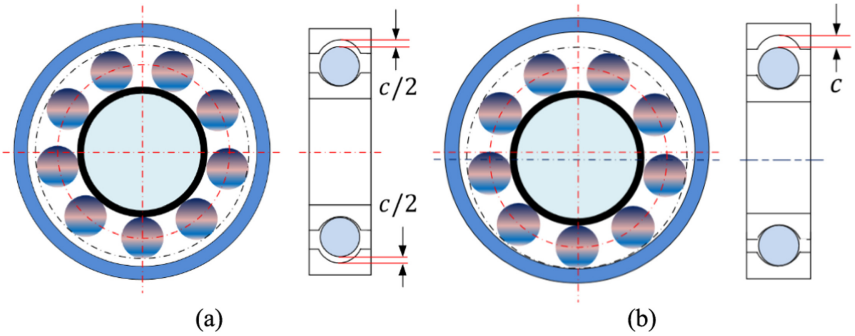

Fig. 1. Schematic diagram of (a) concentric arrangement, (b) initial contact

Table 1. Clearance values of ball bearings under different classes

Bore Diameterd (mm)		C2 (μm)		CN (μm)		C3 (μm)		C4 (μm)		C5 (μm)	
Over	Include	Min	Max	Min	Max	Min	Max	Min	Max	Min	Max
–	2.5	0	6	4	11	10	20	–	–	–	–
2.5	6	0	7	2	13	8	23	–	–	–	–
6	10	0	7	2	13	8	23	14	29	20	37
10	18	0	9	3	18	11	25	18	33	25	45
18	24	0	10	5	20	13	28	20	36	28	48
24	30	1	11	5	20	13	28	23	41	30	53

The bearing dynamic model considering bearing clearances is given in Eqs. (1)–(6).

$$M_s\ddot{X}_s + \sum_{i=1}^{N_b} K[\delta_i]^{3/2} cos\phi_i + \sum_{i=1}^{N_b} C[v_i] cos\phi_i = F, \tag{1}$$

$$M_s\ddot{Y}_s + \sum_{i=1}^{N_b} K[\delta_i]^{3/2} sin\phi_i + \sum_{i=1}^{N_b} C[v_i] sin\phi_i = 0, \tag{2}$$

$$M_h\ddot{X}_h + C_h\dot{X}_h + K_hX_h - \sum_{i=1}^{N_b} K[\delta_i]^{3/2} cos\phi_i - \sum_{i=1}^{N_b} C[v_i] cos\phi_i = 0, \tag{3}$$

$$M_h\ddot{Y}_h + C_h\dot{Y}_h + K_hY_h - \sum_{i=1}^{N_b} K[\delta_i]^{3/2} sin\phi_i - \sum_{i=1}^{N_b} C[v_i] sin\phi_i = 0, \tag{4}$$

$$M_r\ddot{X}_r + C_r\left(\dot{X}_r - \dot{X}_h\right) + K_r(X_r - X_h) = 0, \tag{5}$$

$$M_r\ddot{Y}_r + C_r\left(\dot{Y}_r - \dot{Y}_h\right) + K_r(Y_r - Y_h) = 0, \tag{6}$$

where M, K and C denotes the mass, stiffness and damping, respectively. The subscript s, h and r denote shaft, housing and sensor in the bearing system. ϕ_i represents the angle

position of the i^{th} ball. N_b is the total amount of rolling elements. δ_i and v_i, the nonlinear deformation and velocity of the ith ball, for each rolling element can be obtained by Eq. (7) and (8)

$$\delta_i = \begin{cases} (X_s - X_h)cos\phi_i + (Y_s - Y_h)sin\phi_i - c/2 \times (1 - cos\phi_i) & \delta_i > 0, \\ 0 & \delta_i \leq 0, \end{cases} \tag{7}$$

$$v_i = \begin{cases} \left(\dot{X}_s - \dot{X}_h\right)cos\phi_i + \left(\dot{X}_s - \dot{X}_h\right)sin\phi_i & \delta_i > 0, \\ 0 & \delta_i \leq 0. \end{cases} \tag{8}$$

where c is the bearing internal radial clearance.

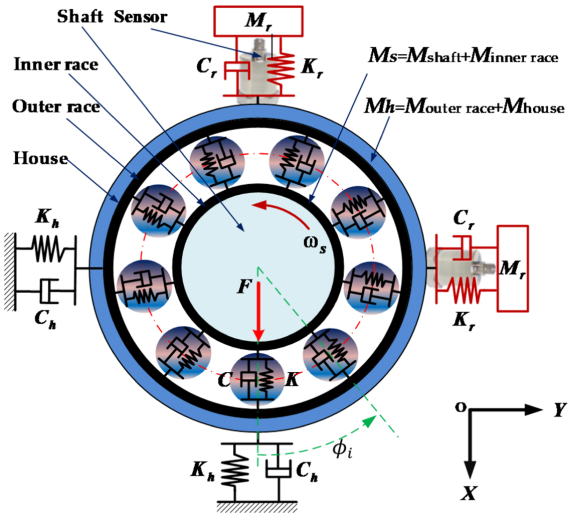

Fig. 2. Schematic diagram of a shaft-housing dynamic model

Based on Hertzian contact theory [9, 17], the total stiffness between inner race and out race can be calculated through Eq. (9). In Eq. (9), K_i, is the Hertzian contact stiffness between the inner raceway and rolling elements, while K_o is the stiffness between outer raceway and balls. In Eq. (10), δ^* means the dimensionless contact deflection, $\sum \rho$ denotes the curvature sum.

$$K = \left[\frac{1}{(1/K_i)^{1/(3/2)} + (1/K_o)^{1/(3/2)}}\right]^{3/2} \tag{9}$$

$$K_{i,o} = \frac{2\sqrt{2}\left(\frac{E}{1-\nu^2}\right)}{3\left(\sum \rho\right)^{1/2}}\left(\frac{1}{\delta^*}\right)^{3/2} \tag{10}$$

Besides, the damping between inner and outer raceway could be obtained through Eq. (11). In Eq. (11), ς means the damping ratio, m_b stands for the mass of each ball.

$$C = 2\,\varsigma\sqrt{m_b \times K} \tag{11}$$

2.3 Bearing Local Defects

Local defects on outer race and inner race are displayed in Fig. 3. In this study, the outer race defect is located at the bottom of the bearing, as shown in Fig. 3(a) and (b). The position of the inner race defect is rotating with the inner race and shaft. The initial position was shown in Fig. 3(c) and (d).

In this study, the defect width W and defect depth was set as 0.8 mm and 0.1 mm, respectively. The additional deflection for outer race and inner race fault could be calculated in Eq. (12).

$$\Delta = \frac{d_b}{2} - \frac{d_b}{2}\cos\left(\frac{\phi_{ball}}{2}\right) = \frac{d_b}{2} - \sqrt{\left(\frac{d_b}{2}\right)^2 - \left(\frac{W}{2}\right)^2} \tag{12}$$

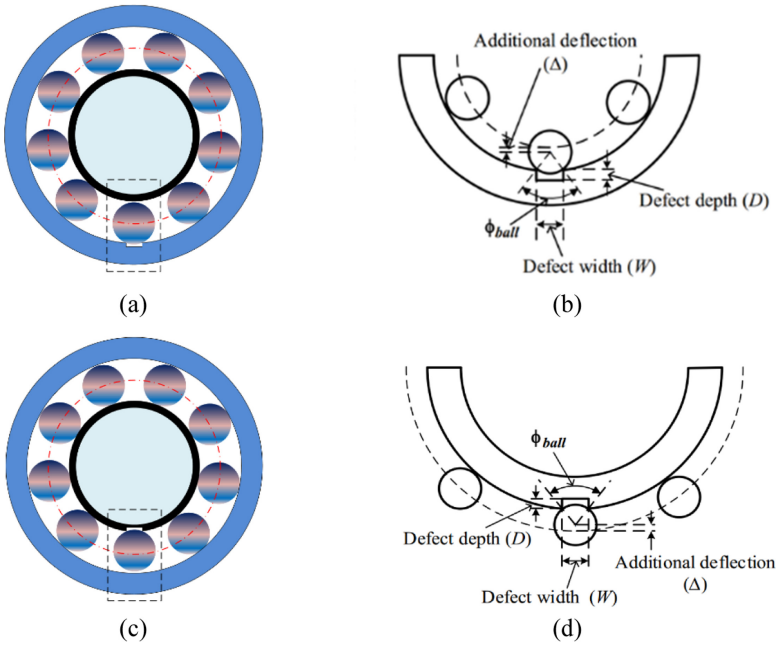

Fig. 3. Local defect: (a, b) outer race defect and (c, d) inner race defect

3 Numerical Simulation Implementation

3.1 Assumptions and Considerations

In this study, to investigate the effect of clearance on vibration characteristics, a dynamic model was established. However, to simplify the question and speed up the numerical solution process, the model was established based on some assumptions and considerations [17], which are list as follow: (1) ideal bearing works under perfect operating

conditions and ignore all manufacturing errors; (2) ignore the influence of temperature and lubrication is sufficient; (3) the contact between the balls and races are pure rolling, i.e., sliding and skidding are ignored in this model.

3.2 Numerical Simulation Implementation

In this study, the numerical simulation was carried out based on bearing 6206. In the dynamic model, the main geometry parameters and the model parameters adopted in numerical simulation are listed in following Tables 2 and 3.

Table 2. Main geometry parameters of 6206.

Notation	Description	Value
d	Nominal bore diameter (mm)	30
D	Nominal outside diameter (mm)	62
d_i	Inner raceway diameter (mm)	37.48
d_o	Outer raceway diameter (mm)	56.45
d_m	Pitch diameter (mm)	46.96
d_b	Ball diameter (mm)	9.485
d_b	Original radial clearance (μm)	0
N_b	Number of rollers	9
α	Contact angle (°)	0

Table 3. Physical properties for simulation study.

Notation	Description	Value
m_s	Mass of shaft (kg)	1.32
m_h	Mass of house (kg)	0.46
m_r	Mass of sensor (kg)	0.02
m_b	Mass of each ball (kg)	2.95×10^{-3}
K_h	Stiffness of house (N/m)	1.2×10^{9}
K_r	Stiffness of sensor (N/m)	4×10^{7}
C_h	Damping of house	939.62
C_r	Damping of sensor	17.89

Except the above parameters, the clearances in this study was set from 0 to 100 μm with the interval as 10 μm, duo to the wear and tear on bearing leads to increase of clearance, which is realized through the change of diameter of races and balls. In the simulation, the shaft rotating speed was arranged as 500 rpm, 1000 rpm and 1500 rpm,

while the external load on the bearing were set from 800 to 4800 N. Besides, the numerical simulation was solved by sub-function of ode15s in MATLAB 2018a.

4 Results and Analysis

4.1 Results

Taking the rotational speed of 1500 rpm, the radial load of 1600 N and the internal radial clearance of 20 μm as an instance, Fig. 4 depicts the vibration waveform, frequency spectrum and envelope spectrum of the X_r. As can be seen, both for bearing with and without local defects, the vibration accelerate displays impulse periodically, but with quite different amplitude. The amplitude of normal bearing is the lowest, while that of bearing with inner race fault is the highest. In addition, from the spectrum, resonant frequency bands could be clearly recognized. As can be seen from envelope spectrum, for bearings both without local defects and with outer race defect, it shows that BPFO and its harmonics are key modulation component. However, for bearing with inner race defect, ball pass frequency of inner race (BPFI), BPFO and rotating frequency (f_r) have the comparatively higher amplitude. The modulation is more complex than normal and outer race defect cases. It may be due to the different location of the inner race defect with the rotation. When the defect is in the load region of the bearing, the defect interacts with the balls and BPFI is significant. While in non-load region, the influence of BPFO exceeds BPFI. Under different rotational speed, the characteristic frequencies, including BPFO, BPFI and f_r of the bearing are shown in Table 4.

Table 4. Characteristic frequency of bearing 6206 under different speed.

Rotational speed (rpm)	Rotating frequency f_r	Cage frequency	BPFO	BPFI
500	8.33	3.33	29.93	45.07
1000	16.67	6.65	59.85	90.15
1500	25	9.98	89.78	135.22

4.2 Comprehensive Analysis

In this section, comprehensive analysis is displayed from time domain and frequency domain. Firstly, statistical indicators from the time domain, such as RMS, kurtosis and entropy, under different radial clearance and eternal load are described in Fig. 5.

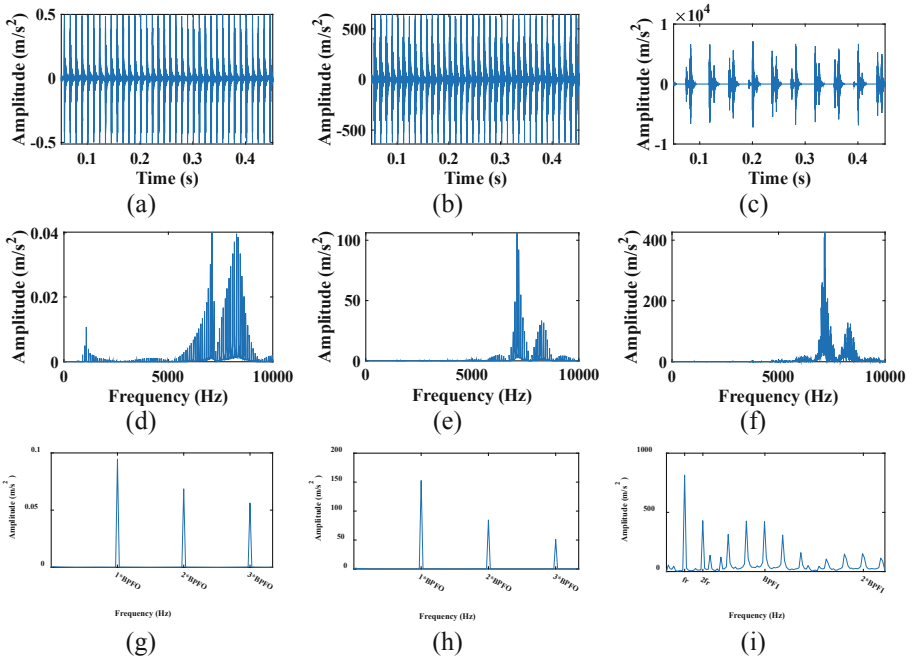

Fig. 4. Results of vibration acceleration (a, b, c), spectrum (d, e, f) and envelope spectrum (g, h, i) of the sensor in *x* direction.

Figure 5 depicts the effect of clearances and load on vibration responses in frequency domain. As can be seen, with the increase of clearances and load, the vibration RMS value shows an uptrend. However, for the normal case, there are several fluctuations from the RMS on both directions of clearances and loads. When there are local defects on outer race, the RMS presents better linear growth trend with the increase of clearances and loads, while RMS values change slightly with clearances under different loads. Besides, kurtosis and entropy fluctuate too much, which brings much difficulty for clearance monitoring of rolling element bearings.

On the other hand, FFT spectrum and envelope spectrum are effective tools from frequency domain to reveal the frequency components. These two spectra were carried out and shown in Fig. 6. It is noted that '800-0' in Fig. 6 stands for 800 N and 0 μm.

From the envelope spectrum, characteristic frequencies of normal bearing and bearing with local defect was extracted, as shown in Fig. 7. As can be seen, when there is no local defect on races, even BPFO is dominant in envelope spectrum, there is no obvious law could be found based on the amplitude of BPFO. However, for bearing with outer race and inner race defect, BPFO and BPFI increases with clearances in general. Especially, BPFO shows an uptrend with the increase of loads in outer race defect case.

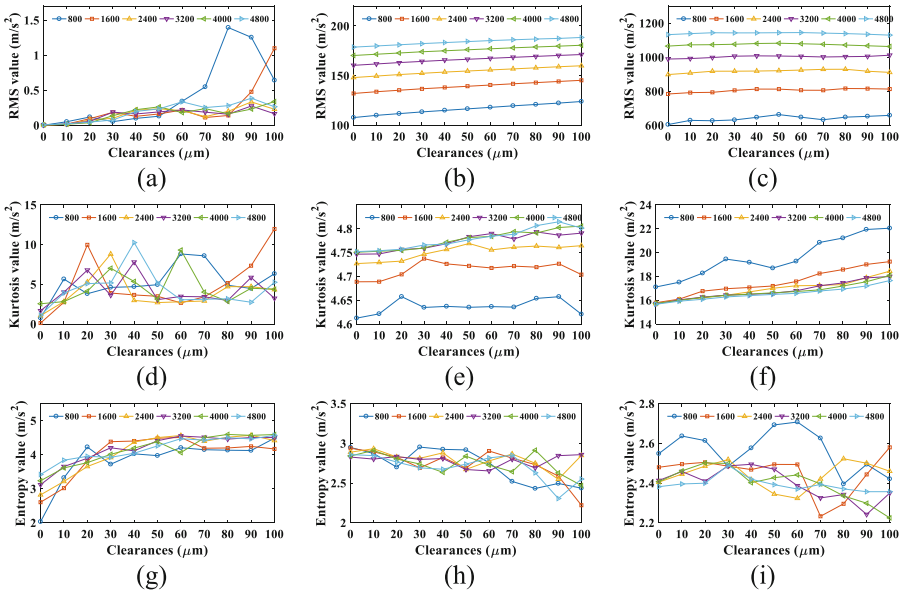

Fig. 5. RMS (a, b, c), kurtosis (d, e, f) and entropy (g, h, i) values under the case of normal (a, d, g), outer race defect (b. e, h) and inner race defect (c, f, i).

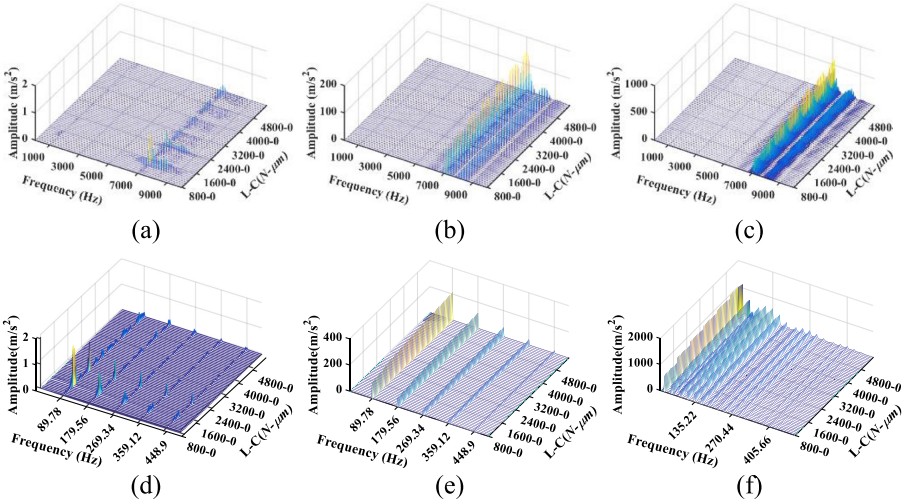

Fig. 6. Spectrum and envelope spectrum of normal (a, d), outer (b, e) and inner (c, f) race defect

But for inner race fault, there are many fluctuations form the BPFI amplitude, which brings difficulties for clearance monitoring and needs special care in detection. In the previous work (Ref. [17]), spectral centroid [22] was utilized to monitor the change of the clearances. The calculation of the spectral centroid is shown in Eq. (13). Based on the spectrum, the spectral centroid values are shown in Fig. 8. As can be seen, the uptrends

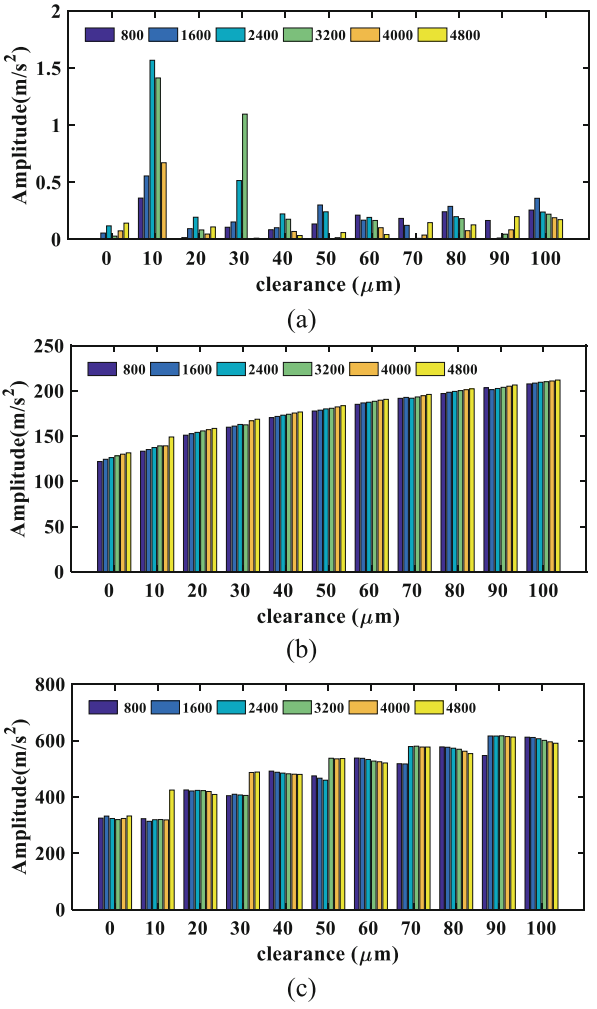

Fig. 7. Characteristic frequency of (a) normal, (b) outer race defect and (c) inner race defect

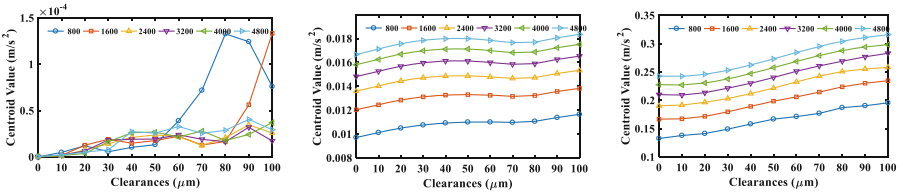

Fig. 8. Spectral centroid of bearing **(a)** normal, **(b)** outer race defect and **(c)** inner race defect

are more clear than statistical indicators in time domain, especially for bearing with local defect, i.e. outer race and inner race defect.

$$Centroid = \frac{\sum_{n=0}^{N-1} f(n)x(n)}{\sum_{n=0}^{N-1} x(n)} \tag{13}$$

5 Conclusion

To investigate the influence of bearing radical clearance when there are local defects on bearing races, this study proposes a nonlinear dynamic model with six DOF, taking into continuously changing clearances and external load. The numerical results show that indicators in frequency domain outperforms statistical indicators in time domain, such as RMS, kurtosis and entropy. Especially, for bearing with local defect on outer and inner races, BPFO and BPFI shows an uptrend with the increase of bearing clearances in general, respectively. However, BPFI of inner race fault fluctuates throughout the clearance, which needs special care in monitoring. Besides, spectral centroid shows good performance on describing the change of bearing clearances except fluctuations in bearing without local defect. All these findings provide theory and data support for bearing clearances monitoring and fault diagnosis at an early stage.

References

1. Wang, Y., Xu, G., Zhang, Q.: Rotating speed isolation and its application to rolling element bearing fault diagnosis under large speed variation conditions. J. Sound Vibr. **348**, 381–396 (2015)
2. Randall, R.B., Antoni, J.: Rolling element bearing diagnostics-a tutorial. Mech. Syst. Sig. Process. **25**, 485–520 (2011)
3. Tse, P.W., Peng, Y.A., Yam, R.: Wavelet analysis and envelope detection for rolling element bearing fault diagnosis—their effectiveness and flexibilities. J. Vibr. Acoust. **123**(3), 303–310 (2001)
4. Lei, Y., Lin, J., He, Z., Zi, Y.: Application of an improved kurtogram method for fault diagnosis of rolling element bearings. Mech. Syst. Sig. Process. **25**(5), 1738–1749 (2011)
5. Samanta, B., Al-Balushi, K.R.: Artificial neural network based fault diagnostics of rolling element bearings using time-domain features. Mech. Syst. Sig. Process. **17**(2), 317–328 (2003)
6. McFadden, P.D., Smith, J.D.: Model for the vibration produced by a single point defect in a rolling element bearing. J. Sound Vibr. **96**(1), 69–82 (1984)
7. Liu, J., Shao, Y., Zhu, W.D.: A new model for the relationship between vibration characteristics caused by the time-varying contact stiffness of a deep groove ball bearing and defect sizes. J. Tribol. **137**(3), 031101 (2015)
8. Halme, J., Andersson, P.: Rolling contact fatigue and wear fundamentals for rolling bearing diagnostics-state of the art. Proc. Inst. Mech. Eng. Part J J. Eng. Tribol. **224**, 377–393 (2010)
9. Harris, T.A.: Rolling bearing analysis. Wiley, Hoboken (2001)
10. Yakout, M., Nassef, M.G.A., Backar, S.: Effect of clearances in rolling element bearings on their dynamic performance, quality and operating life. J. Mech. Sci. Technol. **33**(5), 2037–2042 (2019)

11. Oswald, F.B., Zaretsky, E.V., Poplawski, J.V.: Effect of internal clearance on load distribution and life of radially loaded ball and roller bearings. Tribol. Trans. **55**, 245–265 (2012)
12. Bai, C., Xu, Q.: Dynamic model of ball bearings with internal clearance and waviness. J. Sound Vibr. **294**(1–2), 23–48 (2006)
13. Harsha, S.P.: Rolling bearing vibrations—the effects of surface waviness and radial internal clearance. Int. J. Comput. Methods Eng. Sci. Mech. **7**(2), 91–111 (2006)
14. Upadhyay, S.H., Harsha, S.P., Jain, S.C.: Analysis of nonlinear phenomena in high speed ball bearings due to radial clearance and unbalanced rotor effects. J. Vibr. Control **16**(1), 65–88 (2010)
15. Zhuo, Y., Zhou, X., Yang, C.: Dynamic analysis of double-row self-aligning ball bearings due to applied loads, internal clearance, surface waviness and number of balls. J. Sound Vibr. **333**(23), 6170–6189 (2014)
16. Rehab, I., Tian, X., Gu, F., Ball, A.D.: The influence of rolling bearing clearances on diagnostic signatures based on a numerical simulation and experimental evaluation. Int. J. Hydromech. **1**, 16–46 (2018)
17. Xu, M., Feng, G., He, Q., Gu, F., Ball, A.: Vibration characteristics of rolling element bearings with different radial clearances for condition monitoring of wind turbine. Appl. Sci. **10**(14), 4731 (2020)
18. Zmarzły, P.: Influence of the internal clearance of ball bearings on the vibration level. Eng. Mech. **2018**, 961–964 (2018)
19. Georgiadis, A., Gong, X., Meier, N.: Vibration analysis based on the spectrum kurtosis for adjustment and monitoring of ball bearing radial clearance. In: MATEC Web of Conferences; EDP Sciences, Les Ulis, France (2018)
20. Meier, N., Ambrożkiewicz, B., Georgiadis, A., Litak, G.: Verification of measuring the bearing clearance using kurtosis, recurrences and neural networks and comparison of these approaches. In: Proceedings of the IEEE SENSORS, Montreal, ON, Canada, 27–30 October 2019, pp. 1–4 (2019)
21. Wang, J., Xu, M., Zhang, C., Huang, B., Gu, F.: Online bearing clearance monitoring based on an accurate vibration analysis. Energies **13**, 389 (2020)
22. Schubert, E., Wolfe, J., Tarnopolsky, A.: Spectral centroid and timbre in complex, multiple instrumental textures. In: Proceedings of the International Conference on Music Perception and Cognition, North Western University, Evanston, IL, USA, 3–7 August 2004 (2004)